

1.0-Tb/s/ λ 3840-km and 1.2-Tb/s/ λ 1280-km Transmissions with 168-GBaud PCS-QAM Signals Based on AMUX Integrated Frontend Module

M. Nakamura⁽¹⁾, T. Sasai⁽¹⁾, K. Saito⁽¹⁾, F. Hamaoka⁽¹⁾, T. Kobayashi⁽¹⁾, H. Yamazaki^(1,2), M. Nagatani^(1,2), Y. Ogiso⁽³⁾, H. Wakita⁽²⁾, and Y. Kisaka⁽¹⁾, Y. Miyamoto⁽¹⁾

(1) NTT Network Innovation Laboratories, NTT Corporation, 1-1 Hikari-no-oka, Yokosuka, Kanagawa, 239-0847 Japan

(2) NTT Device Technology Laboratories, NTT Corporation, 3-1 Morinosato-Wakamiya, Atsugi, Kanagawa, 243-0198 Japan

(3) NTT Device Innovation Center, NTT Corporation, 3-1 Morinosato-Wakamiya, Atsugi, Kanagawa, 243-0198 Japan
masanori.nakamura.cu@hco.ntt.co.jp

Abstract: We successfully demonstrate 1.0-Tb/s/ λ 3840-km and 1.2-Tb/s/ λ 1280-km long-haul transmissions in 4.2-THz full C-band 175-GHz-spaced WDM configuration with improving signal noise tolerance using 168-GBaud high-symbol-rate PCS-16QAM and PCS-36QAM signals generated by our AMUX-integrated frontend module. © 2022 The Author(s)

1. Introduction

As communication traffic continues to dramatically increase, large-capacity and cost-effective optical transport networks with digital coherent transceivers have become essential. The transmission capacity per wavelength (capacity/ λ) must be increased to accommodate high-capacity client signals such as the next-generation Ethernet [1] without increasing the number of transceivers. Furthermore, to ensure compatibility with the conventional long-haul network architecture, the transport of 1-Tb/s-class serial data over a distance of 1,000 km is required.

For 1-Tb/s/ λ -class long-haul transmission, the required signal-to-noise ratio (SNR) must be reduced, as a significant optical SNR (OSNR) improvement is difficult due to the limitations of fiber nonlinearity [2]. According to the Shannon theorem, the required SNR to achieve 1-Tb/s for the polarization-division multiplexed (PDM) signal in an additive white Gaussian noise channel changes along with the signal bandwidth corresponding to the symbol rate. The relationship between the SNR and bandwidth is calculated as $\text{SNR} = 2^{C/2B} - 1$, where C is the capacity and B is the signal bandwidth. Figure 1(a) shows the required SNR to achieve 1 Tb/s/ λ as a function of the symbol rate. Probabilistic constellation shaping (PCS) with a probabilistic amplitude shaping (PAS) scheme [3] can approach the theoretical limits with a practical soft-decision forward error correction (SD-FEC) code. Therefore, a high symbol-rate PCS-QAM signal can reduce the required SNR to achieve 1 Tb/s/ λ since it can set various information rates by changing the probability distribution of the constellation points, as shown in Fig. 1(a).

Recently, many 1-Tb/s/ λ -class transmission experiments with high-speed electrical signal generation techniques to overcome the bandwidth limitations of a complementary metal-oxide semiconductor (CMOS) DAC have been reported, as summarized in Fig 1(b) [4–10]. The transmission of 1.3 Tb/s over 200 km was achieved using a 168-GBaud signal with a bandwidth extension scheme utilizing high-speed indium phosphide (InP) technologies [4], and the transmission of 1.6 Tb/s over 153.4 km was achieved using a 128-GBaud signal with a Silicon-Germanium (SiGe) DAC [10]. However, 1-Tb/s/ λ net data-rate long-haul transmission over 1,000 km has not been achieved.

In this paper, we demonstrate 1.0-Tb/s/ λ 3840-km and 1.2-Tb/s/ λ 1280-km transmissions with 168-GBaud PCS-16- and 36-QAM signals based on the AMUX integrated frontend module. The transmission line consists of an 80-km span of pure-silica core fiber (PSCF) and an erbium-doped fiber amplifier (EDFA) with a backward Raman amplifier. The potential spectral efficiencies of the 1.0- and 1.2-Tb/s signals are 5.71- and 6.85-b/s/Hz in a 175-GHz-spaced 4.2-THz full C-band WDM configuration.

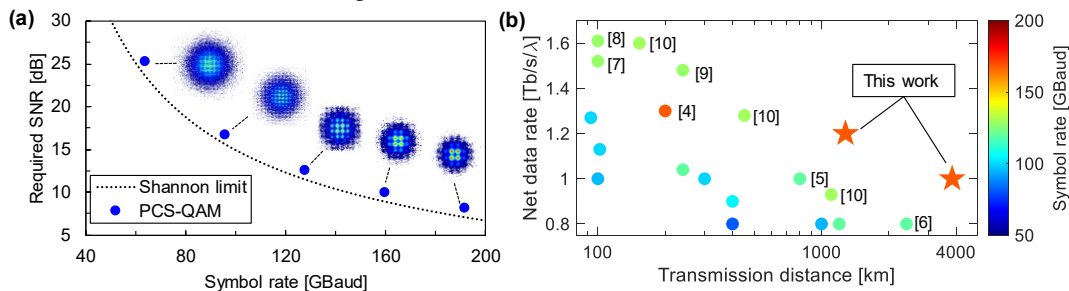


Fig. 1. (a) Required SNR to achieve 1-Tb/s/ λ versus symbol rate and (b) recent transmission experiment results.

2. Long-haul transmission with high-symbol rate signal

The SNR for the optical transmission can be expressed as $1/\text{SNR}_{\text{system}} = 1/\text{SNR}_{\text{TRx}} + 1/\text{SNR}_{\text{Link}}$, where SNR_{TRx} and SNR_{Link} refer to the SNR of the transceiver and of the transmission link, respectively [11]. When the symbol rate increases under a condition of the same signal power, the SNR_{TRx} is degraded, as shown in Fig. 2(a). On the other hand, the SNR_{Link} does not change when the symbol rate is increased in the WDM configuration at the same optical amplification bandwidth at the same input power, as shown in Fig 2(b). Since the SNR_{Link} decreases with the transmission distance, the SNR_{Link} dominates the $\text{SNR}_{\text{system}}$ compared with SNR_{TRx} during long-haul transmission, as expressed in the equation. Therefore, a high-symbol-rate signal with high noise tolerance is suitable for long-haul transmission.

Figure 2(c) shows an example of the dependence of the achievable capacity/ λ on the transmission distance for each symbol rate. The SNR_{TRx} of the 128-GBaud signal is 20.0 dB [8] and that of the 168-GBaud signal is 13.5 dB [4]. The SNR_{Link} is calculated by assuming a 15-dB span loss, 6-dB noise figure of an optical amplifier, and 16-dBm fiber input power of a 4.2-THz WDM signal. Then, the capacities are calculated as $2B \log_2(1 + \text{SNR}_{\text{system}})$. The 168-GBaud signals can achieve a higher capacity/ λ than the 128-GBaud signals when the transmission distance is over 1000 km in this example, as can be seen in Fig. 2(c).

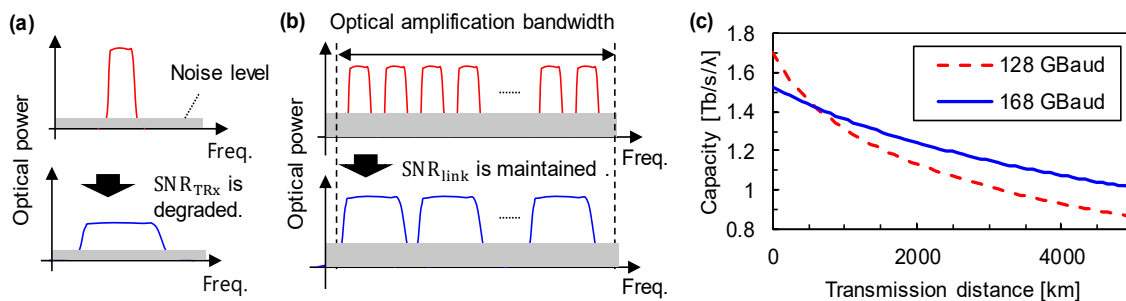


Fig. 2. Effect of symbol-rate increase on signal quality at (a) transceiver and (b) optical amplification in transmission line. (c) Dependence of AIR on transmission distance for each symbol rate.

3. 1- and 1.2-Tb/s long-haul transmission experiments

We evaluated the long-haul transmission performance of 1-Tb/s-class PDM 168-GBaud PCS-QAM signals with an AMUX integrated frontend module. Figure 3(a) shows the experimental setup for the evaluation. The configurations of the transmitter and receiver were the same as those for the 1.3-Tb/s/λ WDM transmission experiments [4] except for the transmission line.

In the transmitter, the AMUX integrated frontend module [12] was used to generate 168-GBaud signals. The module with a 6-dB bandwidth of ~80 GHz consisted of an InP in-phase and quadrature modulator (IQM) and two AMUX drivers (AMUX-DRVs). The AMUX-DRVs operated with 42-GHz clocks double the electrical bandwidth of a 96-GSa/s arbitrary waveform generator (AWG) with a 3-dB analogue bandwidth of 32-GHz. The IQM modulated a 1547.436-nm continuous wave from an integrated tunable laser assembly (ITLA) with a linewidth of ~10 kHz. In the offline transmitter's digital signal processing (DSP), a constant composition distribution matcher and an extended probabilistic amplitude shaping scheme [3] converted a bit sequence derived from the Mersenne Twister into PCS-16QAM and truncated PCS-36QAM [13] signals with a discrete Maxwell Boltzmann distribution. The entropy of the PCS-16- and 36QAM signals was 3.739 and 4.686 bits, respectively. The frame length was 301,056 symbols including 1.64% of pilot symbols. After spectral shaping based on a root-raised cosine filter with a roll-off factor of 0.01, digital pre-equalization was carried out using a fixed linear equalizer [3] to compensate for the frequency response and the in-band crosstalk in the AMUX-DRVs. The high-speed signals were decomposed into two low-speed signals by using the pre-processing for a digital-pre-processed analogue-multiplexed DAC with a half-clock frequency scheme [14]. PDM signals were emulated by using a PDM emulator with a 35-meter delay line (175-ns delay). The interference channel with a 175-GHz grid-spaced 4.2-THz WDM was emulated by an amplified spontaneous emission noise and optical gain equalizer (GEQ) [15]. The signal and interference channel were fed into a flexible grid wavelength selective switch (WSS) for optical equalization (OEQ) to flatten the optical spectrum [3] and to multiplex (MUX) the channels.

The generated WDM signals were launched into a re-circulating loop consisting of two spans of 80-km PSCF, a GEQ to flatten the gain slope, and a loop synchronous polarization controller (LSPC). An EDFA with a backward pumped Raman amplification was used for each 80-km span of PSCF to compensate for fiber loss. The launched power input to the fiber was set to 2 dBm/channel. To obtain a high Raman gain, we used two kinds of PSCFs with

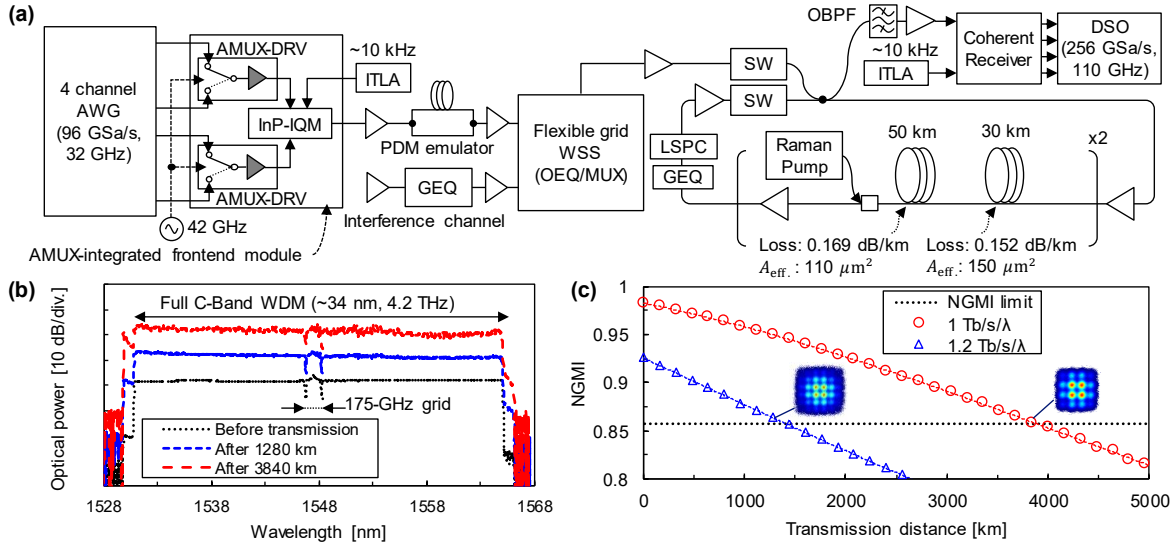


Fig. 3. (a) Experimental setup. (b) Optical spectra before transmission, after 1,280 km, and after 3840 km. (c) NGMI versus transmission distance for 1.2- and 1.0-Tb/s/λ signals.

different effective core areas. The Raman on-off gain was ~ 6 dB at the total pump power of 320 mW. Figure 3(b) shows the optical spectra before and after transmission.

At the receiver side, after being filtered by an optical band-pass filter (OBPF), the signal was detected by a coherent receiver composed of a dual polarization optical hybrid and four 100-GHz bandwidth-balanced photodiodes. The linewidth of the local oscillator input to the optical hybrid from the ITLA was ~ 10 kHz. The signals were digitalized by a 256-GSa/s digital storage oscilloscope with a 110-GHz bandwidth. In the offline receiver's DSP, chromatic dispersion was compensated for by using a fixed equalization. Polarization de-multiplexing and Tx- and Rx-side residual frequency response compensation were achieved by 2048 tap 8×2 multiple-input and multiple-output adaptive equalization using the pilot-symbol-aided least-mean-square algorithm [5]. Frequency offset and carrier phase were compensated for by a pilot-assisted digital phase locked loop [5]. Normalized generalized mutual information (NGMI) [16] was then derived from bit-wise log likelihood ratios (LLRs). Assuming a forward error correction (FEC) code with a 20.94% overhead, which corresponds to a code rate of 0.826 [17], the net rate of the 168-Gbaud PDM PCS-16Q- and 36 QAM signals were 1.0 Tb/s [$2 \times \{3.739 - (1 - 0.826) \times 4\} / 1.0164 \times 168$ Gbaud] and 1.2 Tb/s [$2 \times \{4.686 - (1 - 0.826) \times 4\} / 1.0164 \times 168$ Gbaud], respectively.

Figure 3(c) shows the transmission experimental results of the 1- and 1.2-Tb/s signals. The measured NGMIs of the 1.0-Tb/s signals after 3840-km transmission and 1.2-Tb/s signals after 1280-km transmission were observed to be better than the NGMI threshold of 0.857 for the 20.94% overhead FEC [17], respectively. These results demonstrate that we can achieve 1.0-Tb/s/λ 3840-km and 1.2-Tb/s/λ 1280-km transmission with 168-Gbaud PDM PCS-QAM signals based on the AMUX-integrated frontend module. The potential spectrum efficiencies of the signals in the 175-GHz-grid WDM configuration were 5.71- and 6.85-b/s/Hz, respectively.

4. Conclusion

We have successfully demonstrated 1.0-Tb/s/λ 3840-km and 1.2-Tb/s/λ 1280-km transmissions with 168-Gbaud PDM PCS 16- and 36-QAM signals based on the AMUX-integrated optical frontend module. The potential spectrum efficiencies were 5.71 and 6.85 b/s/Hz in the 175-GHz-grid WDM configuration. These results show that a high-symbol-rate signal can extend the 1-Tb/s/λ-class transmission reach for future optical transport networks.

References

- [1] Ethernet Alliance, "The 2020 Ethernet Roadmap," [online] Available: <https://ethernetalliance.org/technology/2020-roadmap>.
- [2] A. D. Ellis, et al., *J. Lightwave Technol.* 28(4), 423–433 (2010).
- [3] G. Böcherer, et al., *IEEE Trans. Commun.*, 63(12), 4651–4665 (2015).
- [4] M. Nakamura, et al., in Proc. ECOC2019, Tu.2.D.5 (2019).
- [5] T. Kobayashi, et al., in Proc. OFC2019, Th4B.2 (2019).
- [6] M. Nakamura, et al., in Proc. OFC2020, M4K.3 (2020).
- [7] F. Buchali, et al., in Proc. OFC2020, Th4C.2 (2020).
- [8] V. Bajaj, et al., in Proc ECOC2020, Tu1D.5 (2020).
- [9] V. Neskorniy, et al., in Proc OFC2021, Th1A.30 (2021).
- [10] F. Pittalà, et al., in Proc ECOC2021, Th2C1.1 (2021).
- [11] M. Nakamura, et al., in Proc ECOC2021, We3C1.1 (2021).
- [12] M. Nagatani, et al., *IEEE J Solid-State Circuits*, vol. 55(9), 2301–2315 (2020).
- [13] I. Ruiz, et al., *J. Lightwave Technol.* 36(6), 1354–1361 (2018).
- [14] H. Yamazaki, et al., *J. Lightwave Technol.*, 35(7), 1300–1306 (2017).
- [15] J. Elson, et al., *Opt. Exp.*, 25(16), 19529–19537 (2017).
- [16] J. Cho, et al., ECOC2017, M.2.D.2.
- [17] M. Nakamura, et al., in Proc. ECOC2018, We3G.5 (2018).